Supplementary Information Identification of a Triplet-Pair Intermdiate State in Singlet Exciton Fission in Solution.

Hannah L. Stern, Andrew J. Musser, Simon Gelinas,
Patrick Parkinson, Laura M. Herz, Matthew J. Bruzek, John Anthony,
Richard H. Friend and Brian J. Walker.

May 29, 2015

Contents

1 Methods **1**

1.1 Materials 1

1.2 Optical Spectroscopy 1

1.3 Diffusion-Ordered NMR Spectroscopy 3

2 Molar Absorptivity of TIPS-Tetracene **5**

3 Solid-state TIPS-tetracene **6**

3.1 Photoluminescence 6

3.2 Transient absorption 7

4 Photoluminescence Spectroscopy **9**

4.1 Steady-state Photoluminescence 9

4.2 Photoluminescence Up-Conversion Spectroscopy 10

4.3 Photoluminescence Quantum Efficiency (PLQE) and Rate Equations 11
4.3.1 PLQE concentration series 11
4.3.2 Rate equations 12
4.3.3 Rate of excimer formation as a function of concentration 15

5 Transient Absorption Spectroscopy 17
5.1 Singlet exciton decay in dilute solution 20
5.2 Viscosity measurements 20
5.3 Effect of solvent 22

6 Triplet-Exciton Sensitisation and Yield Determination 23
6.1 Triplet Sensitisation 23
6.2 Triplet Exciton Yield 26

7 Spectral De-convolution Techniques 29

8 Three-state model 35

1 Methods

1.1 Materials

TIPS-tetracene was synthesised according to the procedure in reference [1]. This material incorporates two triisopropylsilylethynyl (TIPS) groups coordinated to the para-positions of the second benzene ring in tetracene. These protecting groups enable enable TIPS-tetracene to be far more soluble than unsubstituted tetracene. Solutions of 3- 300 mg/ml (equivalent to 0.005-0.5 molL^{-1}) TIPS-tetracene were prepared in chloroform in an argon environment. For all of the spectroscopic measurements the solutions were measured in a sealed 1 mm path length cuvette. For UV-Vis spectroscopy, the concentrated solutions ($>$ 3 mg/ml) were measured in a 5 μm glass cell with an associated error in the path length of $\sim$0.5 μm.

1.2 Optical Spectroscopy

UV-Vis absorption spectra were measured on a Cary 400 UV-Visible Spectrometer over the photon energy range 1.55 eV-3.54 eV. Steady-state photoluminescence spectra of the solutions were collected using a pulsed laser at 2.64 eV (PicoQuant LDH400 40 MHz) and collected on a 500 mm focal length spectrograph (Princton Instruments, SpectraPro2500i) with a cooled CCD camera. Time-resolved photoluminescence decay of the solutions was measured using both time-correlated single photon counting (TCSPC) and photoluminescence up-conversion spectroscopy (PLUC). The TCSPC set-up uses the same excitation source and camera as the steady-state PL and has a temporal resolution of 300 ps. The excitation source for PLUC set-up was a 100 fs pulse from a Ti:Sapphire laser oscillator (operating at 80 MHz repetition rate). PLUC has a temporal resolution of 200 fs. PLUC signals were measured using up-conversion in a 1 mm thick beta-barium borate (BBO) crystal with a gate pulse. The resulting signal was spatially and spectrally filtered before measurement using the spectrometer and CCD. More sensitive time- and spectrally-resolved photoluminescence measurements were made using an intensified CCD camera. The output of a home built NOPA, a 2.33 eV laser pulse, was used as the excitation source for these measurements. The steady state and time-resolved photoluminescence measurements were conducted with the sample in a side-on excitation geometry to mitigate any self-absorption of the solutions.

The photoluminescence quantum efficiencies of the solutions was measured using an integrating sphere and a 2.33 eV excitation source.

Transient absorption spectra were recorded on a setup that has been previously reported [2]. Spectra were recorded over short (50 fs- 2 ns) and long (1 ns-1 ms) time delays with probe ranges covering from 2.48 eV- 1.55 eV and 1.55 eV- 1.13 eV. For short-time (ps-TA) measurements a portion of the 1 kHz pulses from the central Ti:sapphire amplifier system (Spectra-Physics Solstice) feed into a TOPAS optical parametric amplifier (Light Conversion) to produce a tunable narrowband 2.33 eV pump beam. A second portion is directed into a series of home-built NOPAs, modelled on Cerullo *et al.*[3], to generate probe beams in the visible and near-IR. For short-time measurements the probe is delayed using a mechanical delay-stage (Newport). For long-time (ns-TA) measurements a separate frequency-doubled Q-switched Nd:YVO4 laser (AOT-YVO-25QSPX, Advanced Optical Technologies) is used to generate the pump. This laser produces pulses with a temporal breadth below 1 ns at 2.33 eV and has an electronically controlled delay. The pump and probe beams are overlapped on the sample adjacent to a reference probe beam. This reference is used to account for any shot-to-shot variation in transmission. The sample is held in a 1 mm quartz cuvette, mounted into a holder. The beams are focused into an imaging spectrometer (Andor, Shamrock SR 303i) and detected using a pair of linear image sensors (Hamamatsu, G11608) driven and read out at the full laser repetition rate by a custom-built board from Stresing Entwicklungsburo.

Initial measurements were recorded at a range of laser fluences (5- 1000 $\mu J/cm^2$) on both the ps and ns transient absorption set-ups. The kinetics from these measurements are shown in Figure S12 and Figure S13. The same rate of decay across the fluency series rule out any bi-molecular decay below 1000 $\mu J/cm^2$. The TA spectra presented in this work were recorded at 100-300 $\mu J/cm^2$.

Spectra were also recorded as a function of pump wavelength to determine the possibility and effect of exciting order singlet states. Figure S14 shows the kinetics at 2.0 eV of 300 mg/ml solution pumped with an excitation source of 400 nm, 500 nm and 540 nm. We observe no change in the kinetics and consider that any vibrational relaxation must occur on faster timescales than the tens of ps diffusional timescales we observe for excimer formation.

In all measurements every second pump shot is omitted, either electronically for long-time measurements or using a mechanical chopper for short-time measurements. The fractional differential transmission ($\Delta T/T$) of the probe is calculated for each data point once 500 shots have been collected. Positive signals are due to stimulated emission of excited states (SE). Photoinduced absorptions of excited states (PIA) are observed at lower energies as negative signals.

1.3 Diffusion-Ordered NMR Spectroscopy

Diffusion-ordered spectra were taken using the pulse sequence dstebpgp3s1d. Diffusion constants were calibrated against a sample of methanol in D_2O, whose sample temperature (297.54 K) and viscosity were determined using the difference between the 1H resonances on CH_3 and OH groups[4].

The diffusivity of the molecules in solution at different concentrations is displayed in Figure S1. The diffusion constant of the molecules changed by a small degree over the concentration range (5.0 x $10^{-10}$$m^2s^{-1}$ to 1.2 x 10^{-9} m^2s^{-1}), however this was matched by a change in the diffusivity of the solvent resonance. This is demonstrated in Figure S2, which shows the DOSY diffusion constants for TIPS-tetracene normalised by the diffusion constant for $CHCl_3$, for every sample. While there is still a clear downward trend in the normalised diffusivity as the concentration of the TIPS-tetracene solute increases, this trend is relatively minor compared to the large range of concentrations across the series. Therefore, we assign this change in diffusivity to a change in the viscosity of the solution rather than aggregation of the TIPS-tetracene molecules.

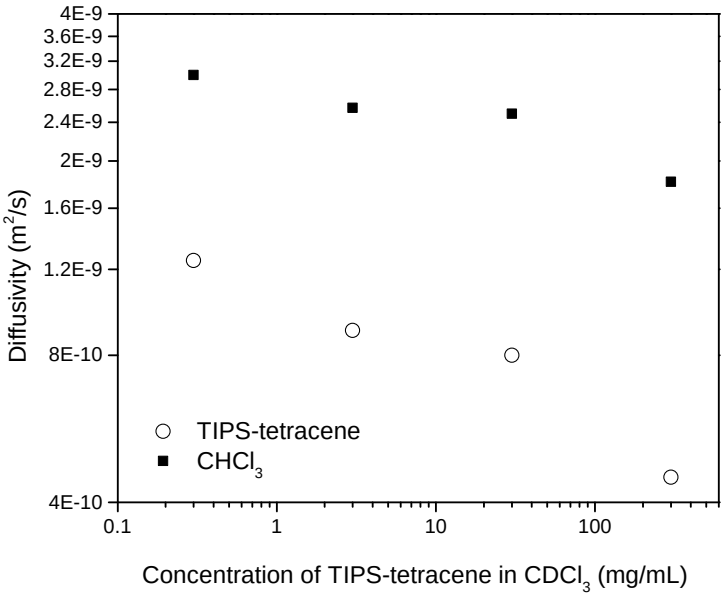

Figure 1: Diffusivity of TIPS-tetracene molecules and $CDCl_3$ molecules, in solutions ranging from 0.3- 300 mg/ml in $CHCl_3$.

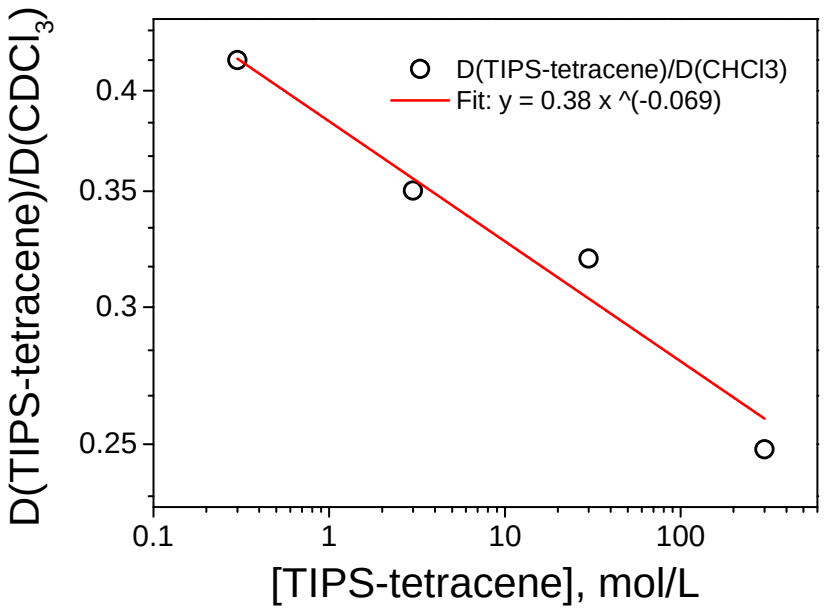

Figure 2: Diffusivity of TIPS-tetracene molecules, normalised by the diffusion constant for $CDCl_3$, in solutions ranging from 0.3- 300 mg/ml in $CHCl_3$.)

2 Molar Absorptivity of TIPS-Tetracene

UV-vis absorption spectra were measured for solutions of 0.3- 300 mg/ml to check for any ground state aggregation of TIPS-tetracene. The 0.3 mg/ml solution was the only solution that did not give an absorbance over 1 in the 1 mm path length cuvette. For all other solutions, cells of path length 5 μm $\pm$ 0.5 μm were used. In Figure S3 the absorption of solutions 3 mg/ml- 300 mg/ml is normalised to the peak value of the 0-2 peak of the 0.3 mg/ml measurement. We observe no broadening or change in peak ratio of the vibronic peaks across the concentrations, indicating that there is no significant aggregation at these concentrations. We note that solutions 100- 300 mg/ml caused saturation of the detector, even in the 5 μm cells, therefore cutting off the tip of the vibronic peaks. The molar absorptivity obtained from the 0.3 mg/ml solution is shown on the right-hand y-axis.

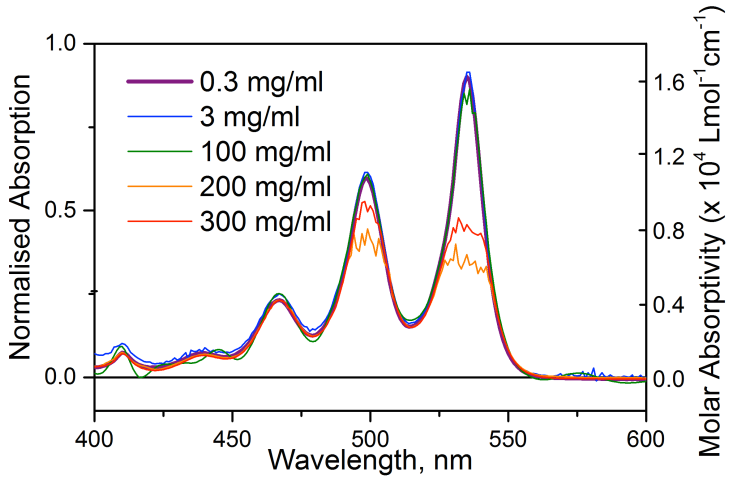

Figure 3: Normalised UV-vis absorption spectra of solutions (0.3- 300 mg/ml in $CHCl_3$).

3 Solid-state TIPS-tetracene

3.1 Photoluminescence

The triplet energy of solid-state TIPS-tetracene was determined by measuring the phosphorescence of a TIPS-tetracene-polystyrene film doped with $Ir(ppy)_3$, following a protocol by Baldo et al[5]. Films were spin coated from solutions of 200 mg/ml polystryrene with 3 wt% TIPS-tetracene and 10 wt% $Ir(ppy)_3$.

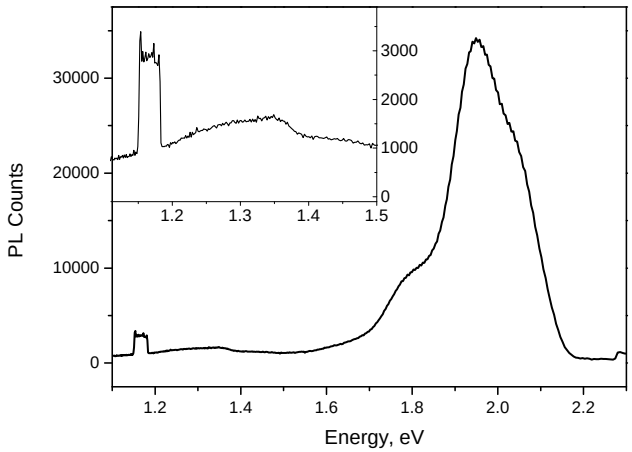

Figure 4: Photoluminescence of a polystyrene (200mg/ml)- TIPS-tetrcacene (6 mg/ml) film. Singlet excitonic emission extends from 1.5- 2.4 eV (580-750 nm). Weak triplet phosphorescence extends from 1.20- 1.35 eV. The peak at 1.18 eV is due to the second harmonic of the excitation source (532 nm laser)

3.2 Transient absorption

A semicrystalline film of TIPS-tetracene, drop cast from 300 mg/ml toluene solution, was measured on the picosecond transient absorption set-up. Figure S6 shows the singlet and triplet time slices from 1 ps to 1 ns. At 1 ps, we observe the singlet absorption analogous to the solution. This species decays to form the triplet (black) which reaches maximum population between 50-100 ps (Figure S7).

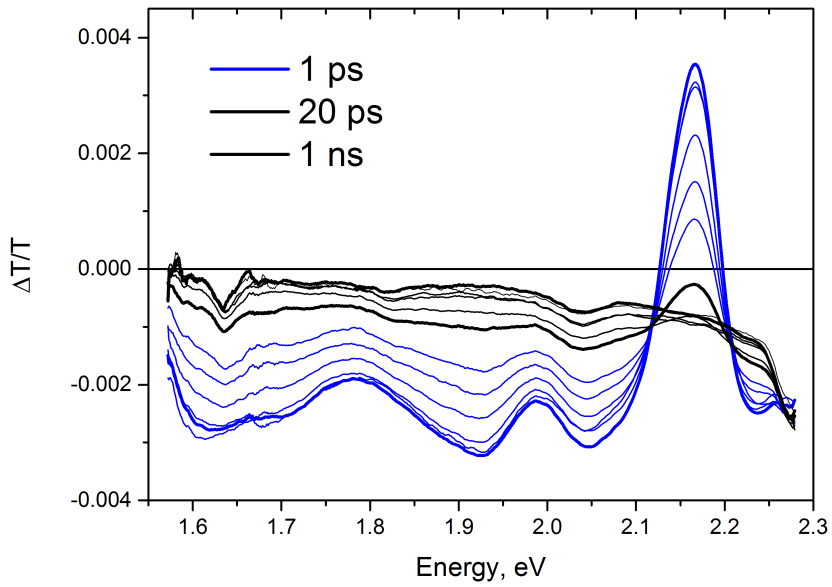

Figure 5: Transient absorption measurement of a semicrystalline TIPS-tetracene film. We observe singlet and triplet species, identical to those observed in the solution. Unlike the solution, we do not resolve an intermediate species.

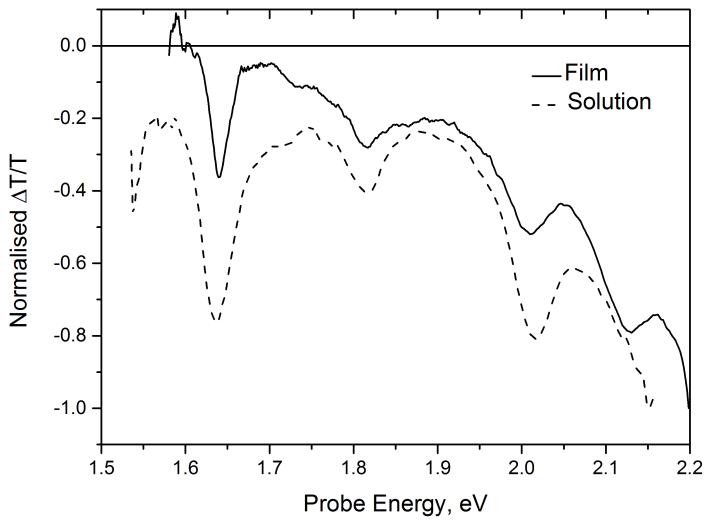

Figure 6: The normalised TA triplet spectra of the drop-cast TIPS-tetracene film and the 300 mg/ml solution.

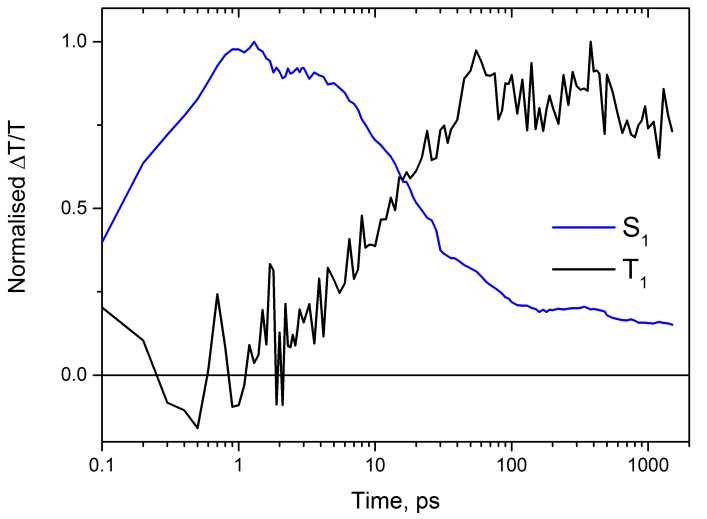

Figure 7: The populations of the singlet and triplet species were resolved for the transient absorption measurement in Figure S6 using the same genetic algorithm code used to analyse the solution measurements. The singlet decays with a ∼15 ps lifetime and the triplet has fully formed by 50-100 ps.

4 Photoluminescence Spectroscopy

4.1 Steady-state Photoluminescence

Figure S8 shows the normalised steady-state photoluminescence spectra of 3 mg/ml, 30 mg/ml and 300 mg/ml solutions. Here we observe the same principal vibronic features at all concentrations. In contrast, only the most concentrated solution displays red-shifted emission that we assign to an excimer. We do not observe a notable change in peak height of the 0-0 vibrational band, which would indicate self-absorption is occurring at the higher concentrations.

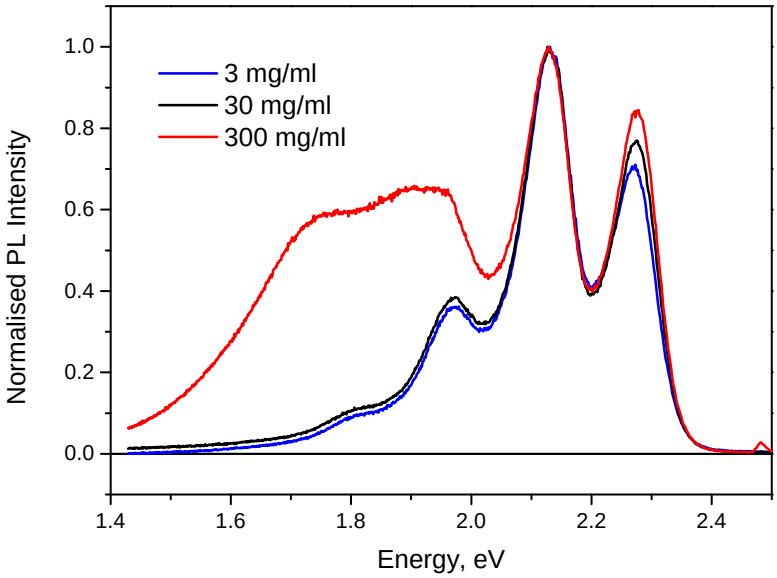

Figure 8: The steady-state photoluminescence of TIPS-tetracene solutions (3 mg/ml- 300 mg/ml in $CHCl_3$.)

4.2 Photoluminescence Up-Conversion Spectroscopy

To determine the sub- 300 ps photoluminescence behaviour, the time-resolved fluorescence of the 300 mg/ml sample was measured using photoluminescence up-conversion spectroscopy (PLUC). This technique has a temporal resolution of ∼200 fs. We observe (Figure S9) a time constant of 148 ps for the decay at 2.18 eV. This lifetime is orders of magnitude shorter than both the excimer lifetime and the arrival of triplet excitons, and supports our conclusion from the TA that singlet excitons decay to form excimers rather than triplet excitons directly.

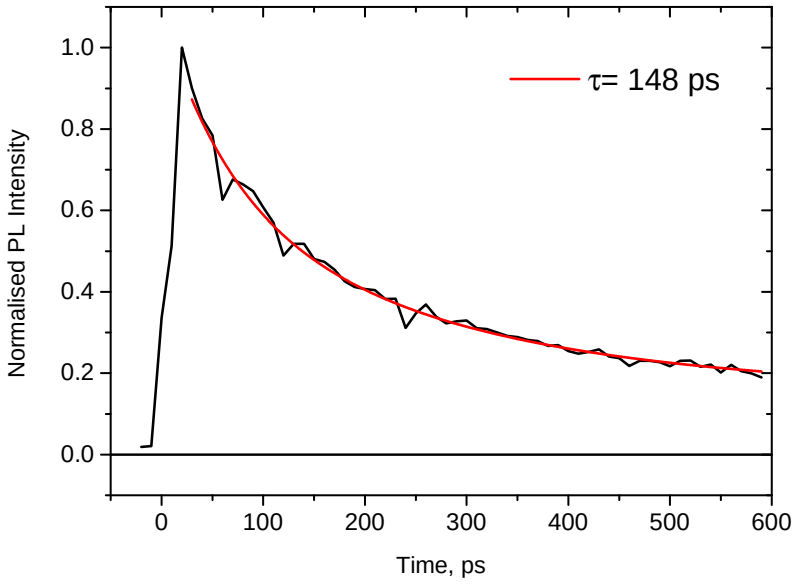

Figure 9: The time-resolved photoluminescence of 300 mg/ml TIPS-tetracene measured using PLUC.

4.3 Photoluminescence Quantum Efficiency (PLQE) and Rate Equations

4.3.1 PLQE concentration series

The PLQE was measured for the solutions and ranged from 75% for 3 mg/ml TIPS-tetracene to 2% in the 300 mg/ml solution. Figure S10 shows the PLQE plotted alongside the singlet lifetime measured at 2.13 eV. We observe a strong correlation between the two quantities. This shows that the difference in PLQE across the solutions is due to the quenching of singlet excitons and any excimeric PL makes a small contribution to the PLQE.

We have considered the possibility that self-absorption affects the absorption efficiencies measured for the solutions. We observe no change in the 0-0/0-1 peak ratio in the steady-state emission of the solutions therefore conclude that any self-absorption present must scale with concentration and thereby give a static offset to the PLQE.

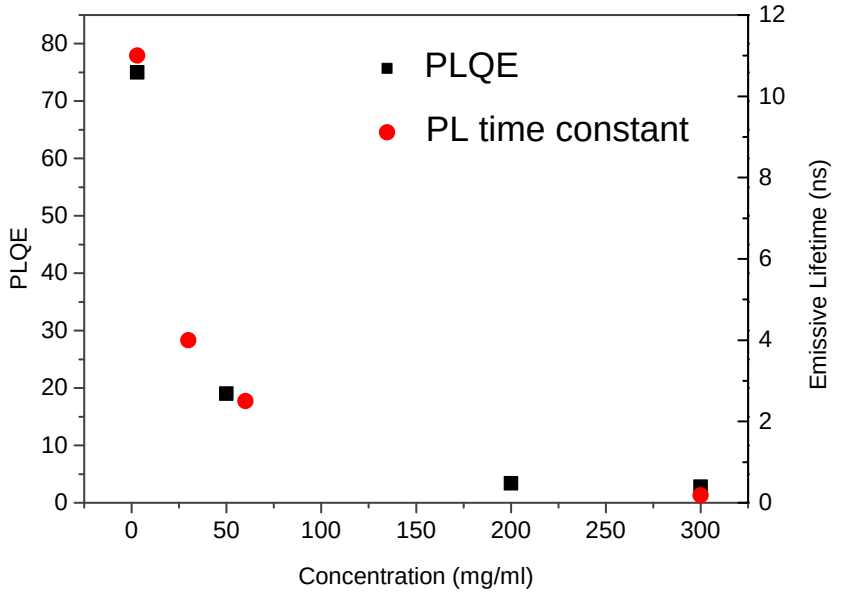

Figure 10: The PLQE of solutions 3 mg/ml - 300 mg/ml plotted alongside the emissive lifetime at 2.13 eV measured using TCSPC.

4.3.2 Rate equations

From analysis of the PLQE and observed radiative decay rates we can compare the instrinsic rates of radiative and non-radiative decay for the singlet (dilute and concentrated) and excimer species*. We obtain the excimer formation rate at 300 mg/ml from the increase in the non-radiative decay of the singlet from the dilute to the concentrated solution. The rate that we obtain is consistent with the time constant for the growth of the excimer that we extract from the transient absorption measurements of the 300 mg/ml solution.

	Singlet (3 mg/ml)	Singlet (300 mg/ml)	Excimer (300 mg/ml)
PLQE	0.75	0.017	0.003
k_{rad} (s^{-1})	6.8 x 10^7	1.8 x 10^{8}*	4.3 x 10^5
k_{nrad} (s^{-1})	2.3 x 10^7	1.41 x 10^{10}	5.7 x 10^7
Intrinsic rad lifetime (ns)	15	5	2300
Formation rate (s^{-1})			1.41 x 10^{10}

The rate of decay of the initially photo-excited singlet excitons in the concentrated solution is given by intrinsic radiative and non-radiative rates of singlet excitons, the rate of excimer formation and the rate of regeneration of singlets from the excimer manifold:

$$\frac{\mathrm{d}S}{\mathrm{d}t} = k_{rad(S)}[S] + k_{nrad(S)}[S] + k_{ef}[S] - k_{sf}[E] \tag{1}$$

where,
$k_{rad(S)}$= the instrinsic radiative rate of the singlet
$k_{nrad(S)}$= the intrinsic non-radiative rate of the singlet
k_{ef} = the rate of excimer formation
k_{sf} = the rate of singlet re-formation from the excimer

The decay of the excimer species is determined by its intrinsic rates of radiative decay and non-radiative decay, the rate of triplet formation, the rate of singlet regenerated and the rate of excimer formation:

$$\frac{\mathrm{d}E}{\mathrm{d}t} = k_{rad(E)}[E] + k_{nrad(E)}[E] + k_{tf}[E] + k_{sf}[E] - k_{ef}[S] \tag{2}$$

*We note that the measured radiative rate of the singlet in the concentrated solution is larger than the dilute solution. We attribute this to the increase in the refractive index of the concentrated solution, which increases the radiative rate of a material in solution [6].

where,
$k_{rad(E)}$= the intrinsic radiative decay rate of the excimer
$k_{nrad(E)}$= the intrinsic non-radiative decay rate of the excimer
k_{tf} = the rate of free triplet exciton formation

The above equations include terms that describe the re-formation of singlet excitons from the excimer manifold. We observe this process via the delayed singlet photoluminescence that decays with the same time constant as the excimeric photoluminescence (Figure 2 in the main text).

We can quantify the percentage of excitations in the system that get converted back to singlet excitons by integrating the singlet exciton photoluminescence over time. When we consider the contribution of the initially photo excited singlet excitons and the re-formed singlet excitons to the overall photoluminescence we find that the delayed emission makes up 1/5 of the singlet's PLQE, thus 0.33% of the PLQE of the whole system. The prompt singlet emission accounts for 1.33% of the PL of the system. This indicates that while 20% of the excitations in the system get returned to the singlet manifold at some time, only 0.33% are permanently lost via singlet emission. We know from the PLQE of the singlet exciton that the majority of the excitations (at least 98.7%) immediately re-form excimers. Emission via the singlet is therefore a minor loss pathway from the excimer manifold.

Thus, to simplify the above equations we can make the approximation that the equilibrium set up between the singlet and excimer is heavily weighted in the direction of excimer formation and the rate of regeneration of the singlet is effectively zero.

The decay of the singlet and excimer populations are approximated as follows:

$$\frac{\mathrm{d}S}{\mathrm{d}t} = k_{rad(S)}[S] + k_{nrad(S)}[S] + k_{ef}[S] \tag{3}$$

To describe the excimer population we can consider two temporal regimes; the growth of the excimer (t $<$ 300 ps) and the decay of the excimer (t $>$ 300 ps). The growth of the excimer is given by the excimer formation rate, which increases with concentration according to second order kinetics (Figure S11). the decay is determined by the radiative and non-radiative rates of the excimer and the triplet formation rate.

when t > 300 ps,

$$\frac{\mathrm{d}E}{\mathrm{d}t} = k_{rad(E)}[E] + k_{nrad(E)}[E] + k_{tf}[E] \tag{4}$$

We obtain the intrinsic non-radiative rate of the excimer and the triplet formation rate from the total non-radiative decay rate of the excimer. As we have a 120% yield of triplet excitons from the excimer, we know that 60% of excimers form triplets and 40% decay via other non-radiative means. Hence, the non-radiative decay of the excimer must be in a ratio of about 2:3 (non-radiative decay: triplet formation). The measured total non-radiative decay rate for the excimer is

$$k_{nrad(E(total))} = 1.42 \times 10^{8} s^{-1} \tag{5}$$

Thus,

$$k_{tf} \sim 8.6 \times 10^{7} s^{-1} \tag{6}$$

$$k_{nrad(E)} \sim 5.7 \times 10^{7} s^{-1} \tag{7}$$

We consider that the long intrinsic radiative lifetime of the excimer gives sufficient time for these non-radiative processes to occur, and hence the efficiency of singlet fission in this system. We have determined that if the excimer radiative lifetime was on the order of the intrinsic radiative lifetime of the singlet, this would reduce the triplet yield from 120% to 60%.

4.3.3 Rate of excimer formation as a function of concentration

We observe that the rate of excimer formation changes as a function of concentration in accordance with second order reaction kinetics. In Figure S11(a) we show the singlet decay and excimer formation of solutions 100-300 mg/ml, alongside the kinetics observed in an amorphous film.

In figure S11(b) the time constant for excimer formation is plotted against 1/concentration. A straight line shows the process follows second order reaction kinetics, indicating a diffusional process. For solutions 100-300 mg/ml this excimer formation time constant was obtained from TA measurements. For solutions 30 and 50 mg/ml the time constant was extracted from the PLQE.

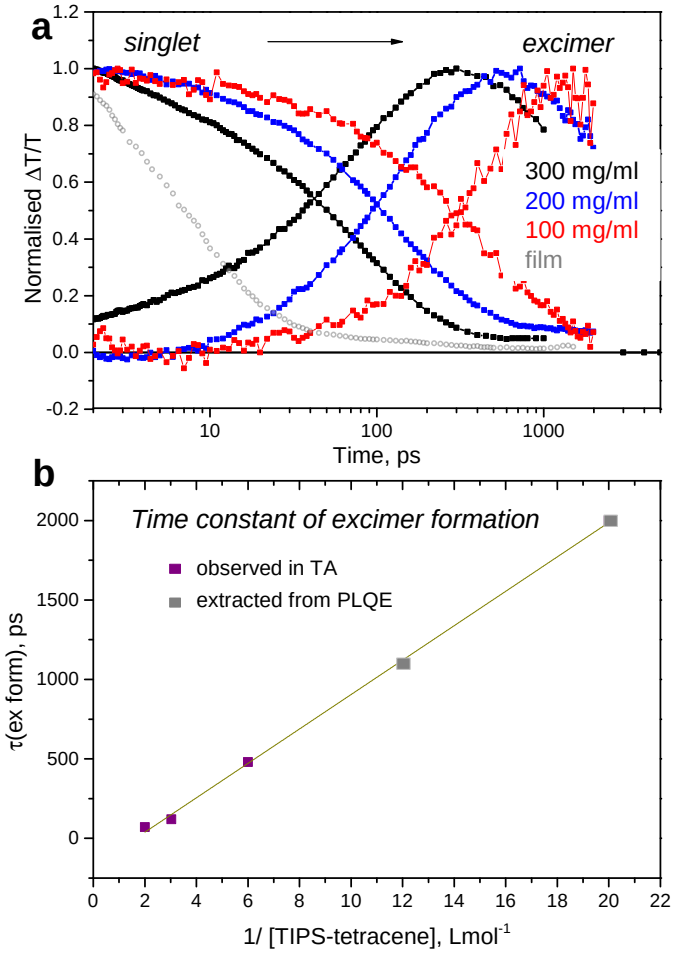

Figure 11: (a) Kinetics obtained from TA measurements of solutions 100-300 mg/ml, as well as the kinetics obtained for the singlet exciton decay in an amorphous film. (b) The time constant of excimer formation plotted against concentration show excimer formation follows second order reaction kinetics. For solutions 100-300 mg/ml the time constants were obtained from the TA measurements, whilst for 30 and 50 mg/ml the time constant were extracted from the PLQE.

5 Transient Absorption Spectroscopy

Transient absorption measurements were recorded at a range of laser fluences (5- 1000 μJ/cm^2) on both the ps and ns set-ups. For both time regimes we observe no fluence dependence across this range, ruling out any bi-molecular decay at these excitation densities (Figure S12) and (Figure S13).

We have also analysed the kinetics as a function of pump wavelength (Figure S14). At 400, 500 and 540 nm we observe to change in the transient absorption spectra. We do not expect that pumping at a shorter wavelength should affect the photophysics of this system, as excitation into any higher lying singlet state should vibrationally relax faster than the diffusional timescales we are observing in the solution system.

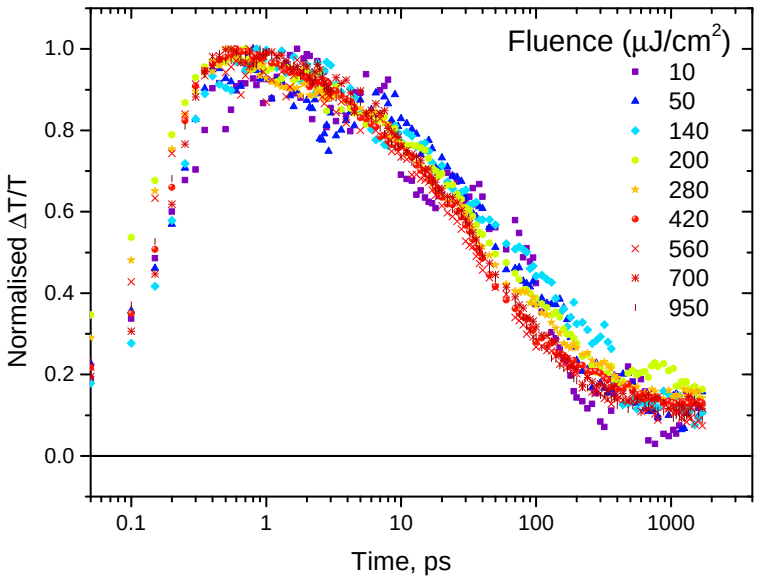

Figure 12: Decay of TA signal at 1.46 eV in a 300 mg/ml solution of TIPS-tetracene at a range of laser fluences, from 50 fs- 1 ns.

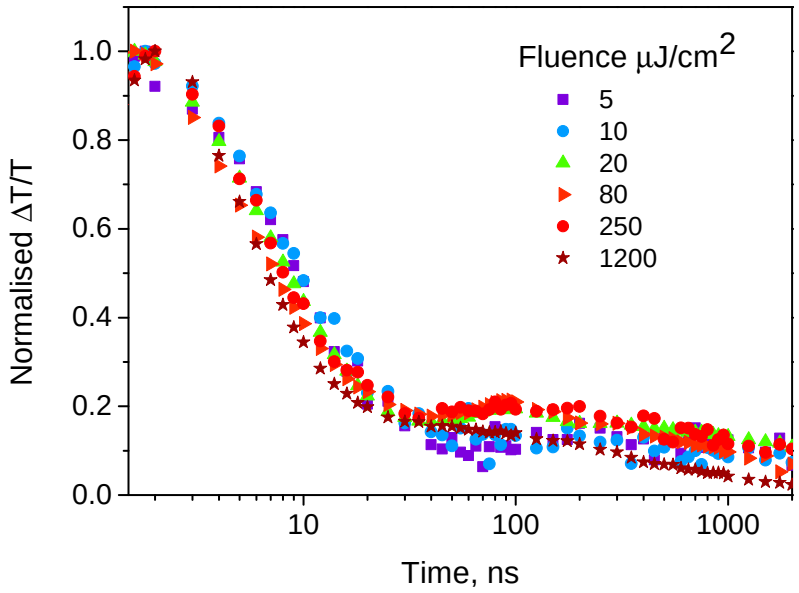

Figure 13: Decay of TA signal at 2.0 eV in a 300 mg/ml solution of TIPS-tetracene at a range of laser fluences, from 1 - 2000 ns.

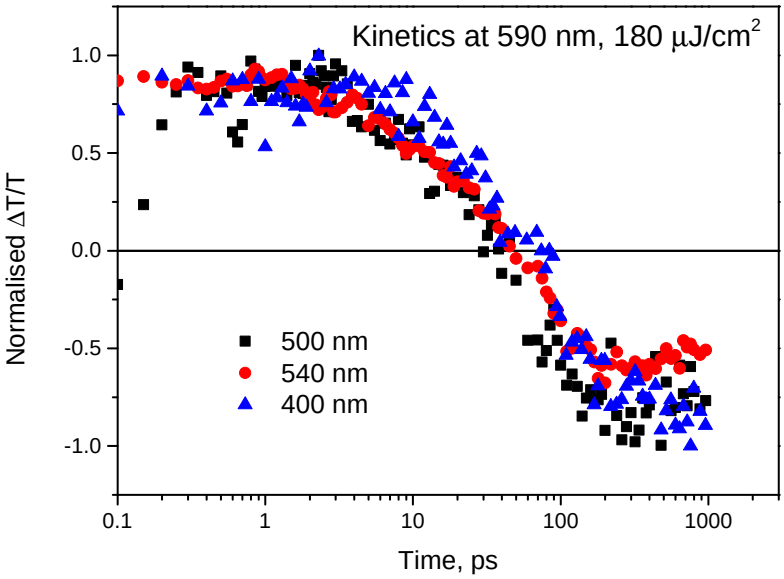

Figure 14: Decay of TA signal at 2.10 eV using pump wavelengths of 400, 500 and 540 nm.

5.1 Singlet exciton decay in dilute solution

The agreement between the decay of the stimulated emission and photoinduced absorption features in the transient absorption measurement with the photoluminescence decay of the dilute solution confirms that only singlet excitons are present in the dilute TIPS-tetracene solution.

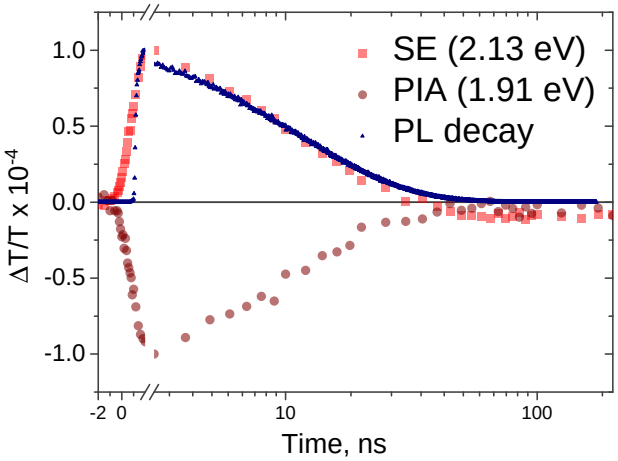

Figure 15: The decay of the stimulated emission and photo induced absorption features in the transient absorption measurement are shown in red. The photoluminescent decay at 2.13 eV of the dilute solution is in blue.

5.2 Viscosity measurements

Solutions of 200 mg/ml TIPS tetracene with varying polystyrene concentrations (125- 500 mg/ml) were measured to observe the effect of a change of viscosity upon the excimer dynamics. Figure S16 shows the kinetic at 2.13 eV, at the peak of the stimulated emission feature. We observe that as the viscosity is increased the decay of the SE and arrival of the excimer PIA is delayed.

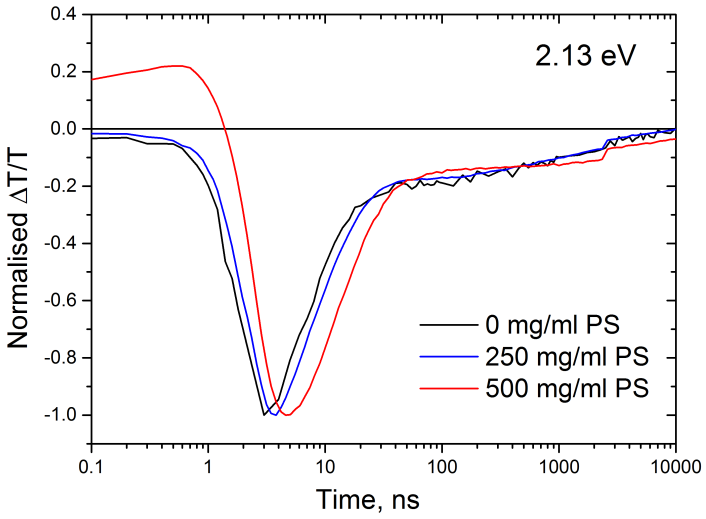

Figure 16: The decay of the stimulated emission feature measured at a range of solution viscosities.

5.3 Effect of solvent

Picosecond transient absorption measurements of TIPS-tetracene in 300 mg/ml toluene solution were carried out in the same conditions as the chloroform measurements. The spectra shows nearly identical singlet and excimer absorption in the different solvents (Figure S17).

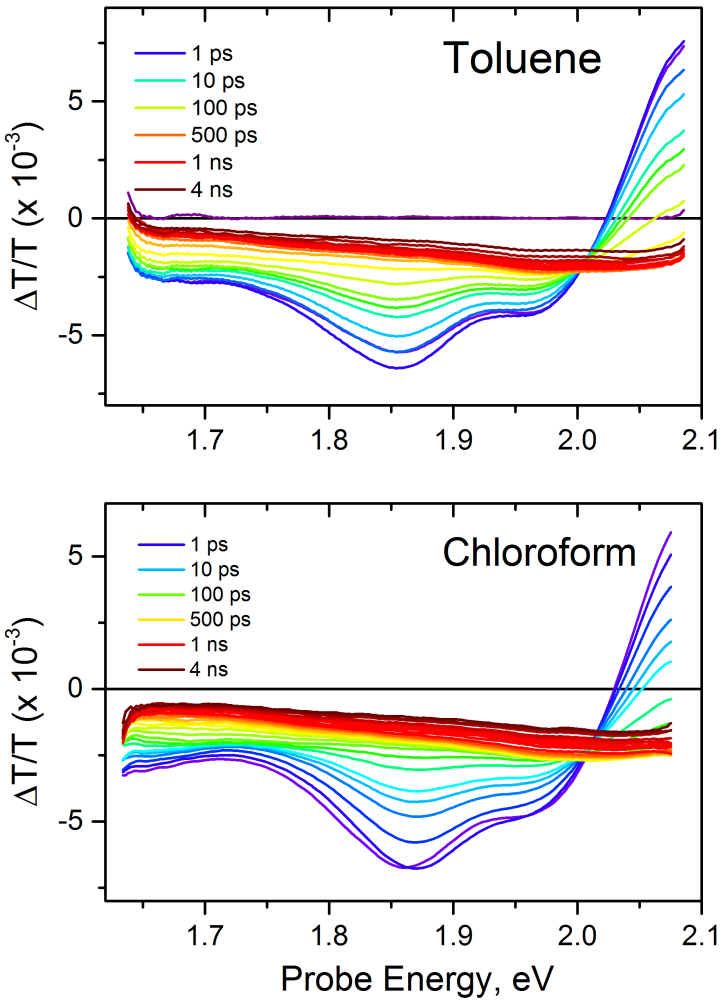

Figure 17: Transient absorption measurement from 1 ps- 4 ns of TIPS-tetracene (300 mg/ml in toluene).

6 Triplet-Exciton Sensitisation and Yield Determination

6.1 Triplet Sensitisation

Following a protocol set out in reference [7] a sensitisation experiment with *N*-methylfulleropyrrolidine was carried out to obtain an absorption spectrum for the TIPS-tetracene triplet exciton. In this experiment the singlet exciton on *N*-methylfulleropyrrolidine is excited directly at 3.49 eV and subsequently undergoes efficient intersystem crossing to form triplet excitons that transfer via diffusion to TIPS-tetracene. Timeslices from 0.1 ns-1500 ns in Figure S18 show the evolution from the singlet exciton on the fullerene, to triplet excitons on the fullerene and finally to form the TIPS-tetracene triplet absorption spectrum. The broad absorption at 1.77 eV is attributed to the fullerene triplet excitons. The TIPS-tetracene singlet absorption spectrum can be observed at early times, superimposed upon the fullerene absorption. Figure S19 shows the population transfer, obtained using a genetic algorithm (see Section 6), resulting from excitation of a mixture of dilute TIPS tetracene and *N*-methylfulleropyrrolidine (1.4 mg/ml TIPS-tetracene and 0.7 mg/ml fullerene) at 3.49 eV.

The spectrum at long-time delays is representative of TIPS-tetracene triplet excitons. We compare this control triplet spectrum to the sharply peaked spectrum we observe at 3 μs in 300 mg/ml TIPS-tetracene (Figure S20) to conclude that triplet excitons are formed at long time delays at that concentration.

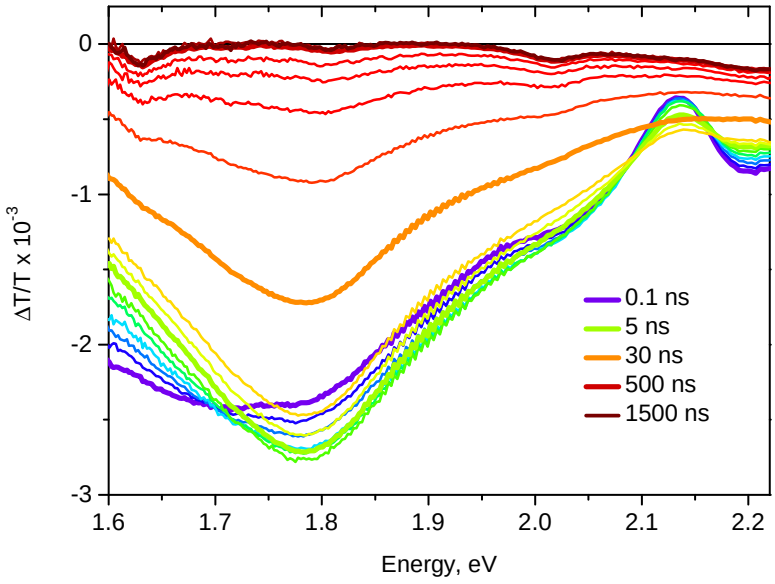

Figure 18: Transient absorption measurement of *N*-methylfulleropyrrolidine (2.8 mg/ml) with TIPS-tetracene (1.8 mg/ml).

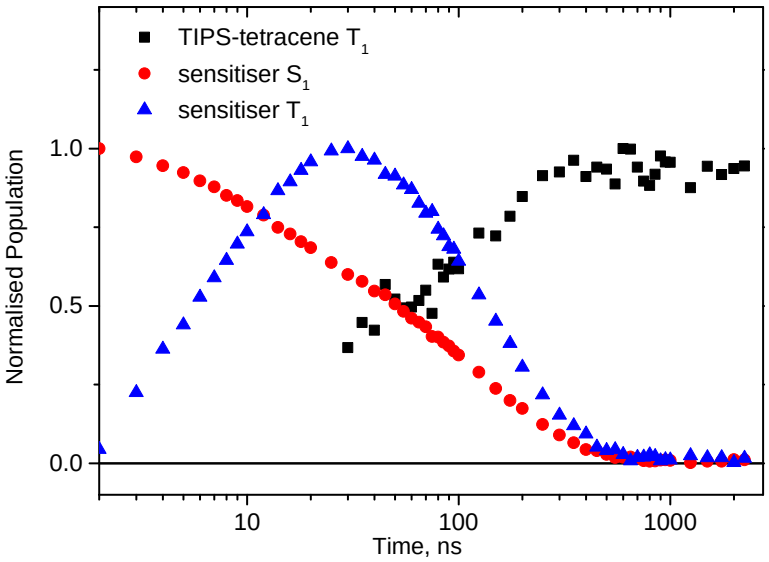

Figure 19: The normalised populations of singlet and triplet excitons on *N*-methylfulleropyrrolidine and the triplet excitons that are formed in dilute TIPS-tetracene.

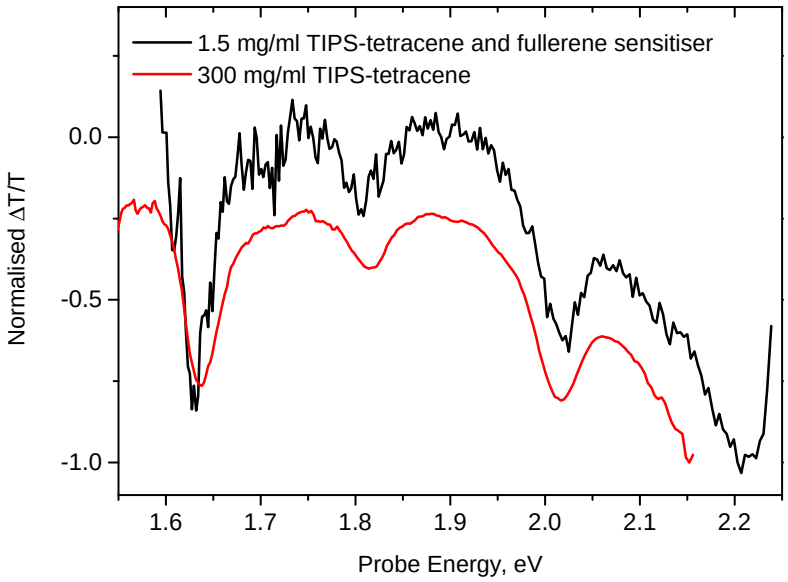

Figure 20: The triplet spectrum from a TA measurement of the concentrated solution (red trace) and the triplet exciton spectrum from the sensitisation experiment (black).

6.2 Triplet Exciton Yield

The extinction coefficient for the TIPS-tetracene triplet excitons is obtained from a sensitisation measurement with *N*-methylfulleropyrrolidine. The triplet lifetime of *N*-methylfulleropyrrolidine (2.4 mg/ml) at 1.77 eV was measured with and without the presence of dilute (1.8 mg/ml) TIPS-tetracene (Figure S21) to determine the rate of triplet transfer to TIPS-tetracene and hence the number of triplet excitons formed on TIPS-tetracene. We attribute any shortening of the sensitiser triplet lifetime in mixed solutions to triplet energy transfer to TIPS-tetracene. The singlet to triplet exciton conversion efficiency in the fullerene sensitiser has been measured elsewhere and is estimated to be between 90-100% [8]. For the rest of our calculations we use the lower limit (90%).The absorption cross section of TIPS-tetracene triplet excitons was determined from the known concentration of TIPS-tetracene excitons formed in the sensitisation measurement and the strength of the triplet absorption. This was used to obtain the number of triplet excitons in the ns-TA TIPS-tetracene measurement and hence the triplet- exciton yield. In concentrated solutions of TIPS tetracene the yield of triplet excitons from singlet excitons is 120%.

TIPS-tetracene singlet exciton concentration following excitation:

$[^1\text{TIPS tetracene}^*] = 1.0 \times 10^{-3}\,\text{molL}^{-1}$ where,

$\frac{Photons}{pulse} = 2.95 \times 10^{11}\text{pulse}^{-1}$

TIPS-tetracene singlet extinction coefficient:

ΔT/T = -0.017 (taken at the peak of the photo-induced absorption signal of the singlet at 1ps following excitation).

$\epsilon^*(^1\text{TIPS tetracene}^*) = 1.41 \times 10^5\,\text{Lmol}^{-1}\,\text{cm}^3$

TIPS-tetracene triplet exciton extinction coefficient:

ΔT/T = -0.00015 (taken at the peak of the triplet absorption at 1.63 eV at 500 ns.)

$\epsilon^*[^3\text{TIPS tetracene}^*] = -5463\,\text{Lmol}^{-1}\,\text{cm}^{-3}$

Concentration of triplet excitons in the 300 mg/ml measurement:

$[^3\text{TIPS tetracene}^*] = 1.2 \times 10^{-3}\,\text{molL}^{-1}$

$[^3\text{TIPS tetracene}^*]/[^1\text{TIPS tetracene}^*] = 1.20$

From the triplet absorption cross section we determined the maximum yield of triplet excitons in the dilute measurement is $< 6\%$ given an average noise level of 0.5 x 10^{-4} (Δ T/T).

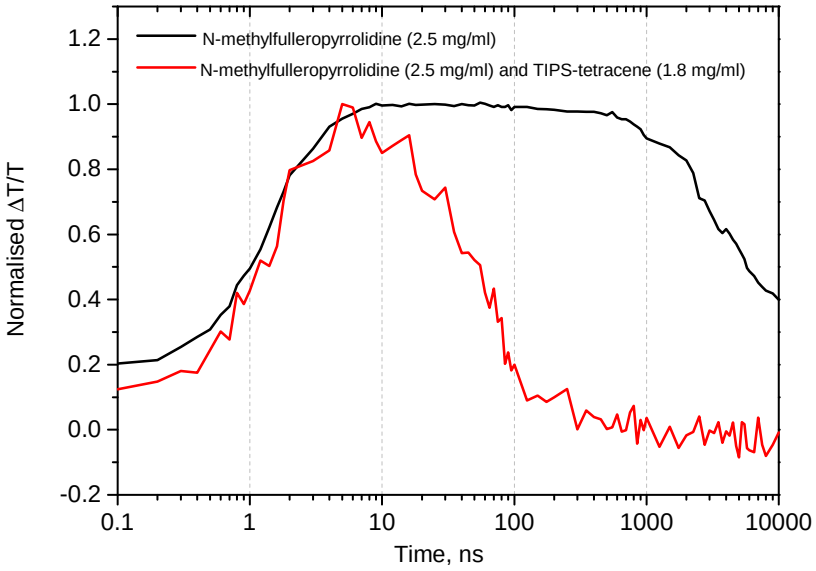

Figure 21: The triplet exciton lifetime on *N*-methylfulleropyrrolidine with and without dilute TIPS-tetracene.

7 Spectral De-convolution Techniques

To identify the spectral species present in the transient absorption measurements of the dilute and concentrated solutions, and to determine their individual evolution over time, we used a combination of singular value decomposition and a spectral de-convolution code [9]. This code generates a given number of spectra that best reproduce the original data, while satisfying basic physical constraints such as spectral shape and population dynamics. The optimisation of these spectra is done by a genetic algorithm. Once the code has minimised the residual between the obtained spectra and the original data the output is a set of spectra and kinetics for the species identified.

The advantage of this optimisation method over other approaches is that the genetic algorithm starts from random initial spectra and does not require a starting kinetic scheme, such as in global analysis methods. In brief, the genetic algorithm is an example of an evolutionary algorithm that factors TA spectra into a pre-determined number of spectral components. The idea is base on natural selection of genes in a population; random spectra or parents are mixed until they give separate spectra that best reproduce the original data, which constitutes a test for genetic fitness.

The advantages of a genetic algorithm for our purpose over other optimisation methods, such as gradient search methods, is that it is more capable of modelling a multidimensional data space that can be noisy and contain several overlapping features. Gradient search methods, on the other hand, are much more likely to get stuck in local minima.

In this work this optimisation code was used to analyse the separate spectral components of the 300 mg/ml TA spectra from both the ps and ns measurements. Singular value decomposition (SVD) was used to give an initial estimation of the number of principal components in each spectrum. From here the code was run to look for the same number of species. It was assumed that the ps-TA measurement would contain primarily singlet and excimer whilst the ns-TA measurement could have contributions from all three species due to the temporal breath of the excitation pulse. For the ns-TA measurements the algorithm was run over 3- 3000 ns, omitting the instrument response region. In these cases no singlet was identified.

Indications of a good fit to the data are reproducibility and good correlation with reference spectra. Once it was determined whether two or three species best fit the data, the genetic algorithm was run several times on the same TA measurement to assess the reproducibility of the results. We assess the reliability of the results of the optimisation by comparing the population decay of the excimer species with the photoluminescence decay (Figure S22). As an additional check, we compare the kinetics of the species identified by the genetic algorithm from the visible and NIR spectral regions that were obtained from four separate measurements (Figure S23).

To determine the variance in the solutions obtained in the optimisation, we determined the spread of possible kinetic and spectral solutions attainable from the output of the algorithm. For the 1-500 ps measurement the singlet and excimer kinetics and spectra are shown in Figures S24 and S23. We observe that in the ps regime there is some variance in the rise of the excimer kinetic, however all solutions show the height of the excimer population at 300-400 ps. The unphysical solutions, i.e. kinetics below zero, are coloured in grey while the solution used in the main figure in the report is in bold. In addition, there is variance in the magnitude of the singlet PIA, but the spectral shape is well defined. The excimer spectrum is best defined in the 1.7-1.85 eV spectral window.

The kinetic solutions for the 1-2000 ns measurement are shown in Figure S26 and Figure S27. The most uncertainty lies in the rise of the triplet kinetic due to the small triplet absorption cross section and the overlap of triplet and excimer absorption features. Beyond 20 ns there is little deviation in the possible solutions. In the spectra we observe variance in the magnitude of the triplet PIA but not in the spectral shape. The spectra obtained by the optimisation agree with the reference spectrum from the sensitisation experiment (in red). There is little variation in the excimer spectrum obtained in the ns-TA measurements, and this shows good agreement to the excimer spectrum from the ps-TA measurement.

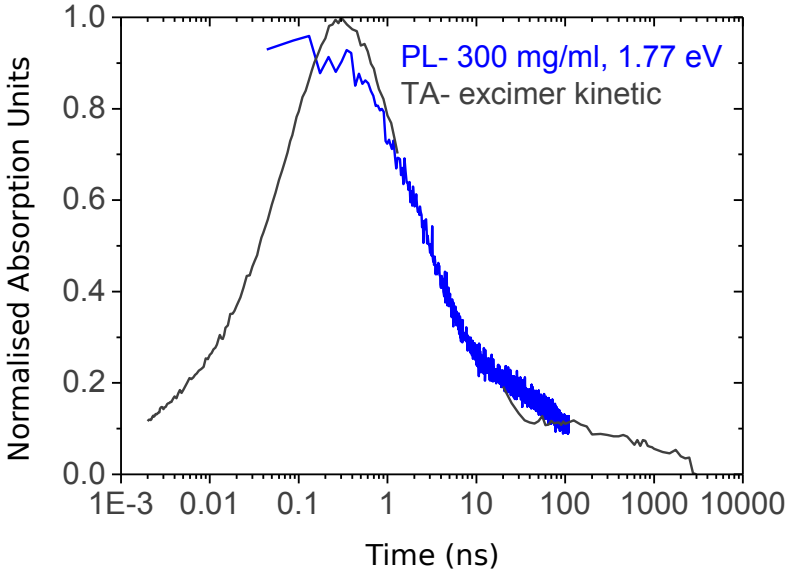

Figure 22: The decay of the excimer species, identified by the genetic algorithm, and the 'excimeric' photoluminescence decay of the concentrated solution.

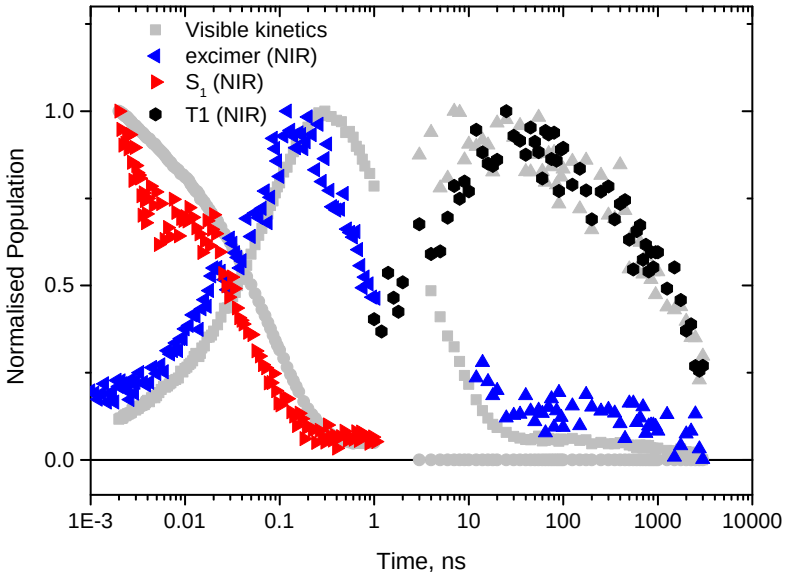

Figure 23: Kinetics of the singlet-excimer-triplet interconversion obtained from measurements in the visible spectral region (grey traces) and near-IR spectral region (coloured).

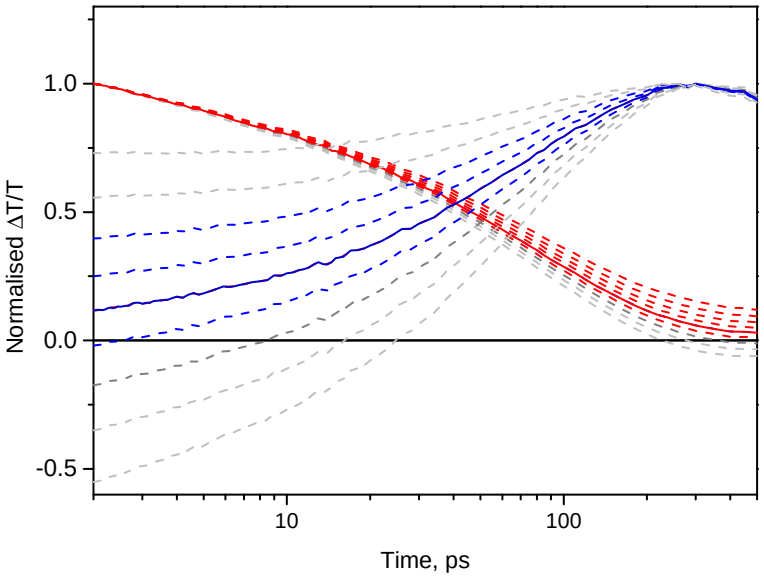

Figure 24: Possible kinetic solutions for the singlet and excimer species for 1-500 ps.

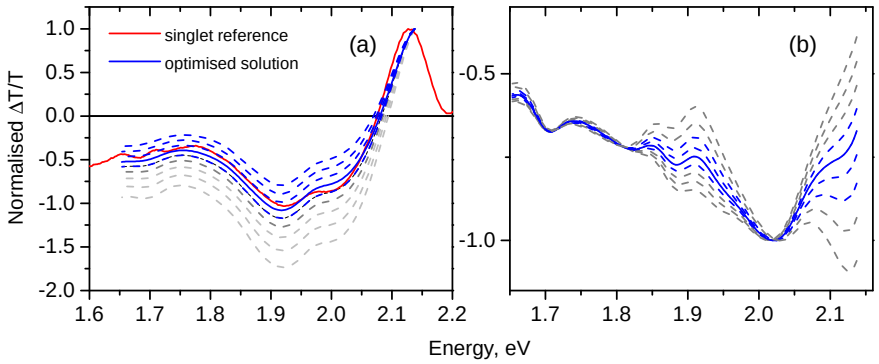

Figure 25: The spread of singlet (a) and excimer (b) spectra associated with the kinetic solutions obtained in the optimisation. The singlet spectrum from the dilute measurement is in red for reference.

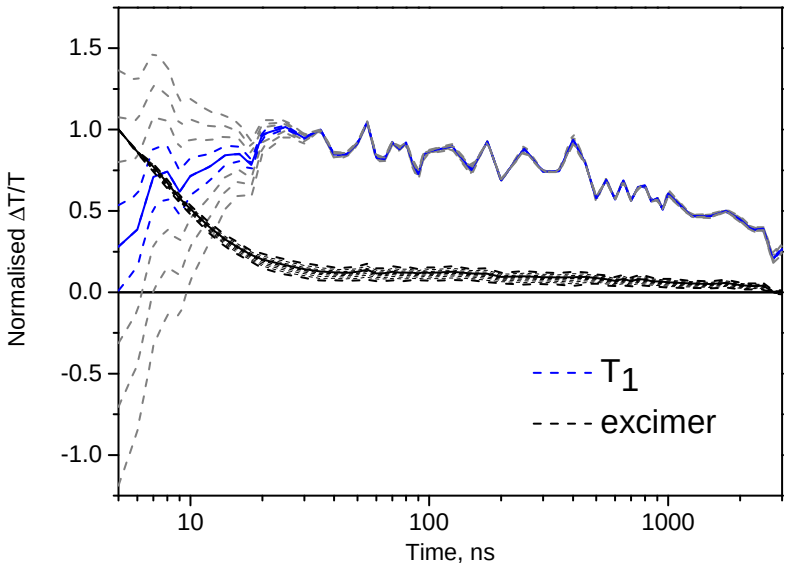

Figure 26: Possible kinetic solutions for the excimer and triplet species for 5- 3000 ns.

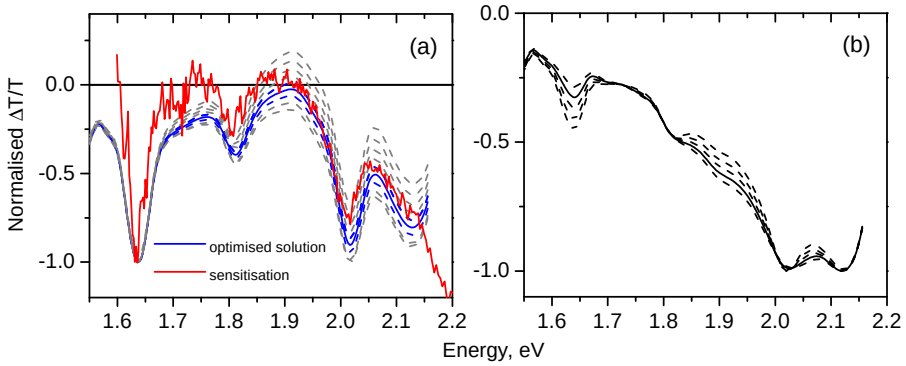

Figure 27: The spread of possible triplet (a) and excimer (b) spectral solutions for 1-2000 ns. The reference triplet spectrum from the sensitisation experiment is shown in red.

8 Three-state model

We consider that our photoluminescence and transient absorption results are consistent with a sequential mechanism of free triplet exciton formation, where dissociation of the excimer leads to two triplet excitons. A parallel pathway is an alternative possibility for triplet formation, whereby excimer and free triplets are both formed directly from singlet excitons and the excimer is not an intermediate in triplet formation. Here we will consider this scenario and highlight why it is less compatible with our results.

The decay of the majority of singlet excitons occurs too rapidly to form triplets on the timescale we observe free triplet exciton formation. The onset of the free triplet exciton absorption occurs after 1 ns, with a time constant of 5 ns and the maximum triplet population between 10-50 ns. If triplet excitons were formed directly from the decay of singlet excitons we would expect to see the singlet exciton population decay with a nanosecond lifetime. In the transient absorption we obtain a $\sim$ 70 ps lifetime for the singlet. This rate is consistent with the rise of the excimer we observe in the transient absorption (55 ps).

A parallel mechanism would give a maximum excimer yield of 40%, given a free triplet exciton yield of 120%. This low excimer yield would require the excimer absorption cross section to be double that of the singlet excitons, in order for the excimer to display equal absorption intensity in the ps transient absorption measurements. In addition, an excimer yield of 40% as a result of a 3:2 (triplet:excimer) branching pathway is unlikely considering the percentage of excitations that undergo singlet regeneration from the excimer manifold ($\sim$ 20%).

References

[1] S. a. Odom, S. R. Parkin, and J. E. Anthony, "Tetracene derivatives as potential red emitters for organic LEDs.," *Organic letters*, vol. 5, pp. 4245–8, Nov. 2003.

[2] A. Rao, M. Wilson, J. M. Hodgkiss, Sei, H. Bassler, and R. H. Friend, "Exciton Fission and Charge Generation via Triplet Excitons in Pentacene/C60 Bilayers," *Journal of the American Chemical Society*, vol. 132, pp. 12698–12703, Aug. 2010.

[3] G. Cirmi, D. Brida, C. Manzoni, M. Marangoni, S. De Silvestri, and G. Cerullo, "Few-optical-cycle pulses in the near-infrared from a noncollinear optical parametric amplifier.," *Optics letters*, vol. 32, pp. 2396–8, Aug. 2007.

[4] E. J. Cabrita and S. Berger, "HR-DOSY as a new tool for the study of chemical exchange phenomena," *Magnetic Resonance in Chemistry*, vol. 40, pp. S122–S127, Dec. 2002.

[5] S. Reineke and M. a. Baldo, "Room temperature triplet state spectroscopy of organic semiconductors.," *Scientific reports*, vol. 4, p. 3797, Jan. 2014.

[6] D. Toptygin, "Effects of the Solvent Refractive Index and Its Dispersion on the Radiative Decay Rate and Extinction Coefficient of a Fluorescent Solute," vol. 13, no. 3, 2003.

[7] A. J. Musser, M. Al-Hashimi, M. Maiuri, D. Brida, M. Heeney, G. Cerullo, R. H. Friend, and J. Clark, "Activated singlet exciton fission in a semiconducting polymer.," *Journal of the American Chemical Society*, vol. 135, pp. 12747–54, Aug. 2013.

[8] P. C. Y. Chow, S. Albert-Seifried, S. Gélinas, and R. H. Friend, "Nanosecond Intersystem Crossing Times in Fullerene Acceptors: Implications for Organic Photovoltaic Diodes.," *Advanced materials (Deerfield Beach, Fla.)*, pp. 4851–4854, June 2014.

[9] S. Gelinas, O. Par, C.-n. Brosseau, S. Albert-seifried, C. R. Mcneill, K. R. Kirov, I. A. Howard, R. Leonelli, R. H. Friend, C. Silva, and S. Centre-ville, "The Binding Energy of Charge-Transfer Excitons Localized at Polymeric Semiconductor Heterojunctions," *The Journal of Physical Chemistry*, vol. 115, pp. 7114–7119, 2011.